J. CHEM. SOC. FARADAY TRANS., 1994, 90(7), 935–939

Appearance Energies of Small Cluster Ions and their Fragments

Brett R. Cameron, Craig G. Aitken and Peter W. Harland*
Chemistry Department, University of Canterbury, Christchurch, New Zealand

Appearance energies of the cluster ions $(CO_2)_n^+$ $(2 \leqslant n \leqslant 4)$, $(N_2O)_n^+$ $(2 \leqslant n \leqslant 4)$ and $(NH_3)_nNH_4^+$ $(0 \leqslant n \leqslant 7)$, and the cluster ion fragments $(N_2O \cdot O)^+$ and $(N_2O \cdot NO)^+$ have been determined by electron impact ionization of neutral clusters formed in a supersonic molecular beam. Results obtained for $(CO_2)_n^+$ $(2 \leqslant n \leqslant 4)$, $(N_2O)_n^+$ $(2 \leqslant n \leqslant 4)$, $(N_2O \cdot NO)^+$ and $(NH_3)_nNH_4^+$ $(0 \leqslant n \leqslant 2)$ are in general agreement with previously reported appearance energies for these species, while the appearance energies of $(N_2O \cdot O)^+$ and $(NH_3)_nNH_4^+$ $(3 \leqslant n \leqslant 7)$ have been measured for the first time. Binding energies deduced from appearance energy measurements for the $(CO_2)_2^+$, $(CO_2)_3^+$ and $(N_2O)_2^+$ cluster ions are observed to be in accord with results obtained using ion–molecule equilibrium methods. Possible mechanisms for the formation of the cluster fragment ions $(N_2O \cdot O)^+$ and $(N_2O \cdot NO)^+$ are discussed.

Atomic and molecular clusters have been the subject of extensive experimental and theoretical research activity for more than 30 years. The fundamental aim of this research effort has been to gain an improved understanding of the evolution from the atomic or molecular properties of a system to its bulk phase properties with increasing cluster size. For example, atomic and molecular clusters represent small, isolated systems which may be used to test and further our understanding of amorphous solids, catalysis, liquid structure and solvation effects. Despite the intensive research activity involved, however, the characterization of cluster species is still in its early stages. Considerably more particle-specific information will be required in order to develop a complete understanding of the mechanisms of cluster formation and elucidate the factors governing the structure and stability of such species. The use of supersonic molecular beams to generate clusters which are rotationally and vibrationally cooled provides a suitable environment for obtaining this information. The essentially collision-free environment of the molecular beam provides the opportunity to investigate the clusters formed in the supersonic expansion in the absence of any further aggregation and problems relating to particle specificity may be largely resolved through the application of ionization and mass-filtering techniques.

In this paper we report an investigation of the appearance potentials for the cluster ions $(CO_2)_n^+$ $(2 \leqslant n \leqslant 4)$, $(N_2O)_n^+$ $(2 \leqslant n \leqslant 4)$ and $(NH_3)_nNH_4^+$ $(0 \leqslant n \leqslant 7)$, and the cluster ion fragments $(N_2O \cdot O)^+$ and $(N_2O \cdot NO)^+$. The chemistry of CO_2 cluster ions is of considerable interest in ionospheric studies of the predominantly CO_2 atmospheres of Mars and Venus,[1] while ammonia clusters are of interest with regard to the energetics of gas-phase proton solvation. Accurate appearance energies are required for the determination of binding energies and enthalpy changes associated with various steps in cluster formation. A knowledge of cluster-ion appearance energies may also be used to obtain information on rearrangement processes and internal cluster ion–molecule reactions which may follow from electron impact or photoionization of neutral clusters. Appearance energies for $(CO_2)_n^+$ $(2 \leqslant n \leqslant 4)$, $(N_2O)_n^+$ $(2 \leqslant n \leqslant 8)$, $(N_2O \cdot NO)^+$ and $(NH_3)_nNH_4^+$ $(0 \leqslant n \leqslant 2)$ have been previously reported,[2–8] while those determined for $(N_2O \cdot O)^+$ and $(NH_3)_nNH_4^+$ $(3 \leqslant n \leqslant 7)$ represent new results.

Experimental

The gas mixture under study was expanded from a high-pressure stagnation reservoir through a commercial electromagnetic pulsed valve (General Valve Corporation, model 9-181) into the first of two differentially pumped vaccum chambers. The valve was modified by the inclusion of a small stagnation volume between the 0.8 mm orifice in the valve and a 50 μm shaped orifice in the exit plate. This gave higher cluster densities than obtained from a valve fitted with a 50 μm orifice. The central core of the pulsed supersonic expansion was sampled by a 1.0 mm skimmer (Beam Dynamics) located *ca.* 300 nozzle diameters (15 mm) from the nozzle exit. The skimmed supersonic beam was allowed to enter the ion source of a Vacuum Generators SXP300 quadrupole mass filter located 10 cm downstream from the skimmer assembly in the second differentially pumped chamber. The electron energy distribution was estimated to be *ca.* 0.85 eV full width at half maximum (FWHM). Output pulses from the channeltron electron multiplier were passed through a high-Q 2 MHz notch filter to eliminate rf pick-up from the quadrupole driver circuitry and amplified with a fast preamplifier followed by an amplifier and pulse amplitude discriminator combination.

The signal-to-noise ratio of the beam signal was optimised using a simple gating arrangement. The TTL output pulses from the pulse-counting preamplifier were split and fed into two and-gates. Using a pulse generator and a pulse delay unit, two 5 V gates of identical width were independently delayed with respect to the nozzle trigger pulse in order to correspond with different regions of the signal pulse envelope. The first window was positioned over the ion arrival time distribution resulting from the pulsed supersonic beam in order to sample signal plus background, while the second was positioned somewhat later in time, sampling only background signal. Output pulses from the two and-gates were counted through a counter-timer. Computer control of electron energy and mass selection was implemented using custom-built 12-bit digital-to-analogue converters incorporated into the mass spectrometer control unit.

The pulsed nozzle was generally operated at a frequency of 10 Hz, with an open time of not more than 2 ms. Background pressures of 10^{-5} and 10^{-8} Torr were maintained in the expansion chamber and the mass spectrometer chamber during normal operation of the nozzle. The temperature of the nozzle was monitored using a thermocouple attached to the body of the valve. The potential difference across the thermocouple was calibrated and amplified using a simple fixed-gain circuit, the output of which was supplied to one of 16 14-bit analogue-to-digital conversion channels monitored. The reservoir pressure was monitored using an MKS Baratron (10000 Torr) connected to an MKS type 286 controller. Experiments were carried out automatically by scanning from low to high and from high to low electron energy

for increments of 0.04 or 0.08 eV. Reproducibility from week to week was excellent and the ionization efficiency curves were automatically analysed using a linear least-squares procedure to locate and tabulate the threshold and any breaks in the curves. All of the ionization efficiency curves reported were calibrated against argon and the molecular ion recorded simultaneously.

Results

Neutral CO_2, N_2O and NH_3 clusters were produced by expanding gas mixtures containing 100 Torr of argon and 500 Torr of CO_2, N_2O or NH_3 made up to a total pressure of *ca.* 4000 Torr with helium at a reservoir temperature of 295 K. These mixtures were found to produce supersonic beams of sufficiently high cluster content for reliable determination of appearance energies for the cluster ions $(CO_2)_n^+$ $(2 \leqslant n \leqslant 4)$, $N_2O_n^+$ $(2 \leqslant n \leqslant 4)$ and $(NH_3)_nNH_4^+$ $(0 \leqslant n \leqslant 7)$. For the N_2O mixture it was also possible to determine the appearance potentials for the cluster ion fragments $(N_2O \cdot O)^+$ and $(N_2O \cdot NO)^+$. While monomer and cluster speed distributions were not measured, we would expect the parallel translational temperature of the cluster beams to be close to the value of *ca.* 6 K measured previously for a pure helium beam under the same source conditions.[9] The extent of rotational cooling which occurs during the supersonic expansion of these gas mixtures is unclear and will depend on the efficiency of rotational to translational energy transfer in collisions between the molecules and clusters and the rare-gas atoms. We tentatively suggest that the terminal rotational temperatures of the molecules and clusters will be less than 40 K in all cases. No clusters containing helium or argon atoms were observed for any of the gas mixtures examined.

Ion counts were measured at up to 100 points with a typical counting period of 5 s at each electron energy repeated some 15 to 20 times to obtain an average count with an acceptable standard error. Average ion counts were also recorded at an electron energy of 70 eV at the beginning and end of each run. Depending upon the number of ions examined, a run could take up to 3 or 4 h to complete and it was therefore necessary to consider any potential sources of long-term experimental instability that might adversely affect the accuracy of the measurements. In particular, it is known that the cluster content of supersonic molecular beams is highly sensitive to variations in source pressure and temperature,[10] and these variables were carefully monitored throughout each run. Owing to the small flow of gas through the 50 μm nozzle, the reservoir pressure was observed to drop by not more than 2 or 3% over a 4 h period of continuous operation and no change in nozzle temperature was detected.

The semi-log plot method[11,12] has been used in this study to determine the cluster-ion appearance potentials with an estimated accuracy of ±0.1 eV in all cases. This error limit includes both statistical and systematic errors. Although nominally less accurate than ideal photoionization measurements, reproducibility is excellent and certainly good enough to allow critical comparisons to be made between our results and those of previous experimental and theoretical investigations. The appearance potential of Ar^+ used as the primary electron energy scale calibrant for all of the appearance potential measurements was taken to be 15.76 ± 0.01 eV.[13]

CO_2 Clusters

Illustrative examples of ionization efficiency curves measured for $(CO_2)_2^+$, $(CO_2)_3^+$ and $(CO_2)_4^+$ are shown in Fig. 1, where every second point has been omitted for clarity. Calibration of the electron energy scale was achieved through a concurrent measurement of the ionization energy for Ar^+. The corrected values of the $(CO_2)_2^+$, $(CO_2)_3^+$ and $(CO_2)_4^+$ appearance energies and the calculated binding energies are shown in Table 1 with literature values for comparison.

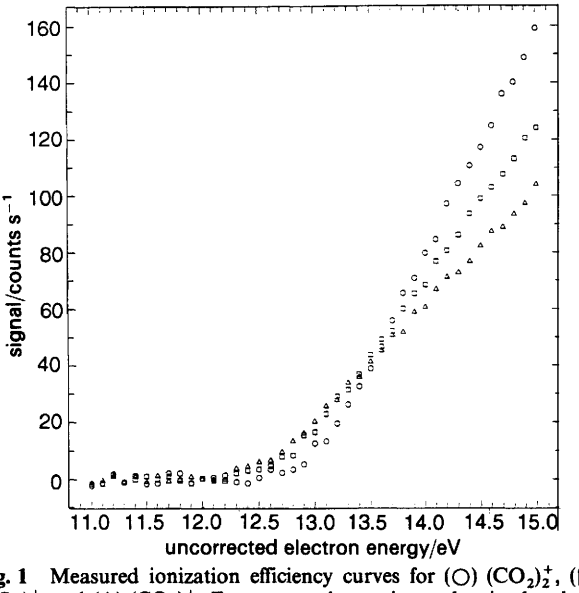

Fig. 1 Measured ionization efficiency curves for (○) $(CO_2)_2^+$, (□) $(CO_2)_3^+$ and (△) $(CO_2)_4^+$. Every second experimental point has been omitted for clarity.

N_2O Clusters

Ionization efficiency curves for $(N_2O)_n^+$ $(2 \leqslant n \leqslant 4)$ and the cluster ion fragments $(N_2O \cdot O)^+$ and $(N_2O \cdot NO)^+$ are illustrated in Fig. 2 and 3. The appearance energies determined for these species are summarized in Table 2. The value of 12.3 eV determined for the appearance energy of $(N_2O)_2^+$ is in

Table 1 Appearance energies (E_{app}) and binding energies (E_b) for $(CO_2)_n^+$ $(2 \leqslant n \leqslant 4)$

		E_b/eV for $(CO_2)_{n-1}^+ \cdot CO_2$	
ion	E_{app}/eV	this work	literature
$(CO_2)_2^+$	13.1 ± 0.1	0.73	0.675[a,b] 0.564[a,c]
$(CO_2)_3^+$	12.8 ± 0.1	0.36	0.32[b]
$(CO_2)_4^+$	12.6 ± 0.1	0.26	0.22[d]

[a] These values have been corrected to 0 K by Linn and Ng[4] and are therefore lower than the values stated by the authors. [b] Ref. 14. [c] Ref. 1. [d] Ref. 15.

Table 2 Appearance energies (E_{app}) and binding energies (E_b) for N_2O clusters

		E_b/eV	
ion	E_{app}/eV	this work	literature
$(N_2O \cdot O)^+$	14.6 ± 0.1		
$(N_2O \cdot NO)^+$	14.3 ± 0.1		
	17.0 ± 0.2		
$(N_2O)_2^+$	12.3 ± 0.1	0.61	0.56[a] 0.57[b,c]
$(N_2O)_3^+$	12.1 ± 0.1	0.22	
$(N_2O)_4^+$	12.0 ± 0.1	0.12	

[a] Ref. 4. [b] Ref. 18. [c] Corresponds to a temperature of 481 K and may not be directly comparable.

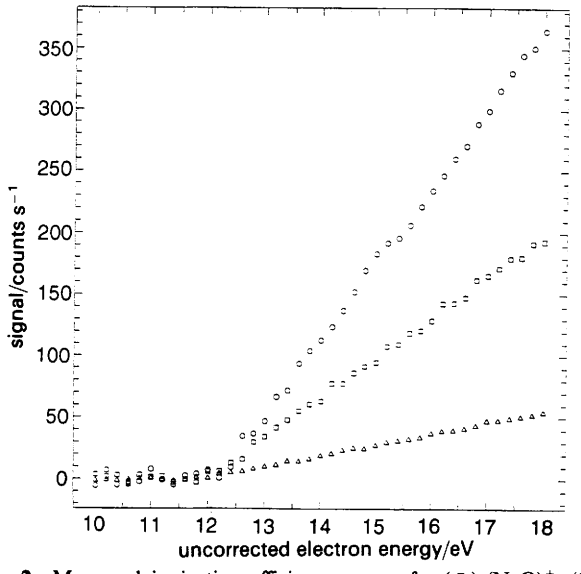

Fig. 2 Measured ionization efficiency curves for (○) $(N_2O)_2^+$, (□) $(N_2O)_3^+$ and (△) $(N_2O)_4^+$. Every second experimental point has been omitted for clarity.

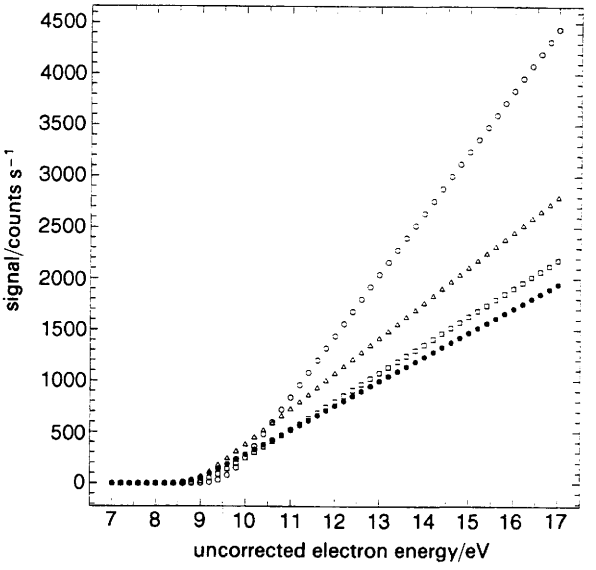

Fig. 4 Measured ionization efficiency curves for (○) NH_4^+, (□) $(NH_3)NH_4^+$, (△) $(NH_3)_2NH_4^+$ and (●) $(NH_3)_3NH_4^+$. Every second experimental point has been omitted for clarity.

excellent agreement with that of 12.35 ± 0.02 eV reported by Linn and Ng[4] and the value of 12.394 ± 0.015 eV reported by Kamke *et al.*[6] It can be seen from Fig. 4 that the shape of the ionization efficiency curve measured for the $(N_2O \cdot NO)^+$ cluster ion fragment is significantly different to the shape of the curves obtained for any of the other ions illustrated in Fig. 1–5. Apart from the ionization threshold at 14.3 eV, there is a sharp change of slope at *ca.* 17.0 eV, suggesting the presence of a second threshold for the formation of this ion. The shape of this curve was found to be totally reproducible. The $(N_2O \cdot NO)^+$ ion was also observed by Linn and Ng,[4] who estimated an appearance energy of 14.01 eV, in reasonable accord with the lowest-energy threshold of 14.3 eV determined in the present study. A second threshold at *ca.* 17.2 eV is also apparent on the $(N_2O \cdot NO)^+$ photoionization efficiency curve recorded by Linn and Ng. Although they attempted no interpretation of this, it lends support to our observation of a reproducible, higher-energy threshold. The appearance energy for the cluster fragmentation product $(N_2O \cdot O)^+$ has not been previously reported. In view of the agreement observed between the appearance energies of $(N_2O)_2^+$ and $(N_2O \cdot NO)^+$ determined in the present study and those obtained by Linn and Ng[4] using photoionization, we might expect the appearance energies of 12.1, 12.0 and 14.6 eV obtained for $(N_2O)_3^+$, $(N_2O)_4^+$ and $(N_2O \cdot O)^+$, respectively, to be equally reliable.

The appearance energies for $(N_2O)_3^+$ and $(N_2O)_4^+$ reported in the photoionization study of Kamke *et al.*[6] are 12.29 ± 0.02 and 12.26 ± 0.04 eV, respectively, or *ca.* 0.2 eV higher than the electron impact threshold reported here and listed in Table 2. Although, in principle, photoionization should yield more accurate thresholds with lower uncertainty, experimental photoionization data do not often measure up to these expectations. The appearance energies

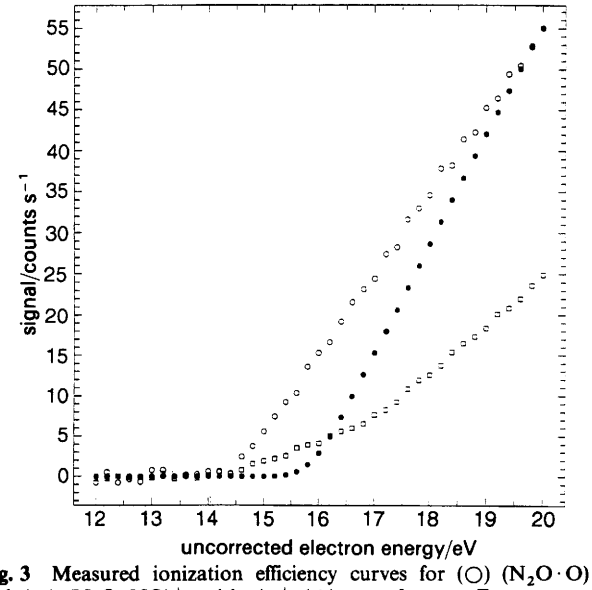

Fig. 3 Measured ionization efficiency curves for (○) $(N_2O \cdot O)^+$ and (□) $(N_2O \cdot NO)^+$, with Ar^+ (●) as reference. Every second experimental point has been omitted for clarity.

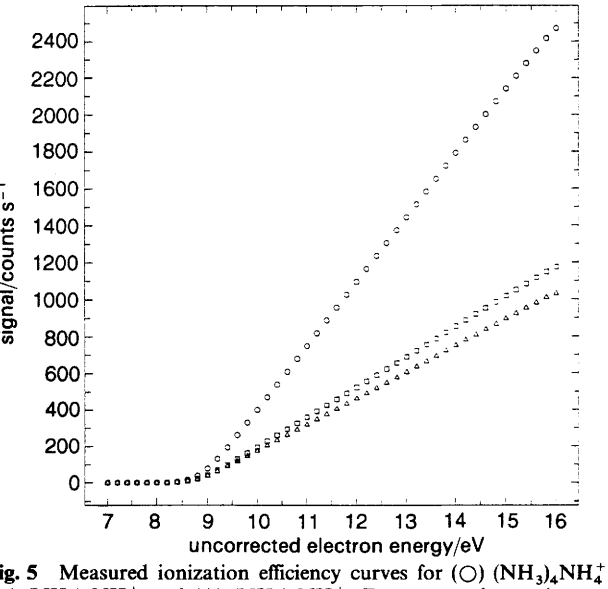

Fig. 5 Measured ionization efficiency curves for (○) $(NH_3)_4NH_4^+$, (□) $(NH_3)_5NH_4^+$ and (△) $(NH_3)_6NH_4^+$. Every second experimental point has been omitted for clarity. The ionization efficiency curve for $(NH_3)_7NH_4^+$ would be superimposed on that for $(NH_3)_6NH_4^+$ and has been omitted from the figure. The higher signal level for $(NH_3)_4NH_4^+$ over its neighbours, $(NH_3)_3NH_4^+$ (Fig. 5) and $(NH_3)_5NH_4^+$, reflects the higher stability of this cluster.

for the $(N_2O)_n^+$ $(1 \leqslant n \leqslant 8)$ cluster ions are reported by Kamke *et al.*[6] with experimental uncertainties from ± 0.015 eV for $n = 2$ to ± 0.04 eV for $n = 8$. However, inspection of the experimental data shown in Fig. 1 of ref. 6 for the $(N_2O)_n^+$ ions shows little correspondence between the reported values and the thresholds anticipated from the data. The threshold regions are smeared, noisy and the shape of the curves varies considerably from $n = 1$ to $n = 8$. The reported thresholds and uncertainties are the result of an empirical multi-parameter fitting procedure, which cannot gurantee a unique solution. So, despite photoionization thresholds quoted to two or three decimal places with uncertainties in the meV range, some consideration must be given to the data treatment. Electron impact ionization thresholds do return reliable values within the stated uncertainty, although it must be acknowledged that recoil energy and internal excitation in the ionization process are folded into the absolute values measured by either technique.

Using the appearance energy value of 12.3 eV measured for $(N_2O)_2^+$ with the ionization energy of 12.886 ± 0.002 eV for N_2O[16] and the estimated intermolecular binding energy of 0.02 eV for the neutral dimer,[17] the bond dissociation energy of $(N_2O)_2^+$ has been calculated to be 0.61 eV, in good agreement with the value of 0.56 eV reported by Linn and Ng[4] and the value of 0.57 eV determined by Illies[18] using ion–molecule methods. Note, however, that this latter value relates to a measurement of ΔH° for the association reaction of N_2O and N_2O^+ at 481 K and therefore may not be directly comparable. The $(N_2O)_2^+$ binding energy calculated using the photoionization data reported by Kamke *et al.*[6] would be 0.512 eV, which seems a little low. Assuming the same binding energy of 0.02 eV for $(N_2O)_3$ and $(N_2O)_4$, we calculate bond dissociation energies of 0.22 and 0.12 eV for $(N_2O)_2^+ \cdot N_2O$ and $(N_2O)_3^+ \cdot N_2O$, respectively, compared with values of 0.124 and 0.05 eV calculated using the photoionization thresholds reported by Kamke *et al.*[6]

The appearance energy of 14.6 eV determined for the $(N_2O \cdot O)^+$ cluster ion fragment is observed to be 2.3 eV greater than that of $(N_2O)_2^+$, close to the difference of 2.4 eV between the appearance energy of N_2O^+ from N_2O (12.886 eV) and the appearance energy of O^+ from N_2O (15.29 eV).[16] This observation may be rationalized by writing the structure of $(N_2O \cdot O)^+$ as $O^+ \cdot N_2O$ and to postulate that the formation of this species involves the ionization and fragmentation of one of the N_2O monomer units in $(N_2O)_2$ without any significant perturbation of the accompanying cluster molecule. Note that the same argument would also apply to the species $(CO \cdot CO_2)^+$ and $(NH_2 \cdot NH_3)^+$ observed by Stephan *et al.*[5,7] An alternative mechanism proposed by them for the formation of these cluster fragment ions involved an internal ion–molecule reaction. If the ion within the $(N_2O)_2$ cluster is initially formed in some electronically excited state N_2O^{+*}, then the $(N_2O \cdot O)^+$ ion may be produced by the following sequence of reactions:

$$(N_2O)_2 + e^- \rightarrow N_2O \cdot N_2O^{+*} + 2e^- \rightarrow N_2O_2^+ + N_2 \quad (1)$$

The $N_2O_2^+$ species produced in this manner would be expected to have an appearance energy greater than that of $(N_2O)_2^+$ by at least the additional energy required for the electronic excitation of the parent ion. Irrespective of whichever mechanism applies, we can use the measured appearance potential of 14.6 eV for $(N_2O \cdot O)^+$, the thermochemical threshold of 15.29 eV for the formation of O^+ from N_2O[16] and the binding energy of 0.02 eV for $(N_2O)_2$[17] to estimate a lower bound of 0.71 eV for the bond dissociation energy of $(N_2O \cdot O)^+$.

The lowest energy threshold observed for the formation of $(N_2O \cdot NO)^+$ corresponds to an appearance energy of 14.3 eV, while the break at higher electron energy equates to an ionization threshold of *ca.* 17.0 eV. Note that the differences of 2.0 and 4.7 eV observed between these thresholds and the appearance energy of 12.3 eV obtained for $(N_2O)_2^+$ correspond very well to the differences of 2.124 and 4.854 eV between the ionization energy of 12.886 eV for N_2O^+ and the thermochemical thresholds of 14.19 and 17.76 eV for the fragmentation processes

$$N_2O + e^- \rightarrow NO^+(X\,^1\Sigma^+) + N(^4S) + 2e^- \quad (2)$$

and

$$N_2O + e^- \rightarrow NO^+(X\,^1\Sigma^+) + N(^2P) + 2e^- \quad (3)$$

respectively.[16] Applying the same argument used for $(N_2O \cdot O)^+$, it seems reasonable to write the structure of $(N_2O \cdot NO)^+$ as $NO^+ \cdot N_2O$ and to describe the formation of this species as involving the ionization and fragmentation of one of the N_2O molecules in the neutral dimer without any significant perturbation of the other. Realistically, the molecules making up a cluster must exert an influence on one another. This might well be expected to include a lowering of the ionization energy with increase in cluster size, as observed in this and other studies. This adds support to the mechanism of cluster ionization described above. Linn and Ng[4] observed that the photoionization efficiency curve they measured for $(N_2O \cdot NO)^+$ had essentially the same profile as that of NO^+ produced from the fragmentation of N_2O^+. Such an observation indicates that the fragmentations of N_2O^+ and $(N_2O)_2^+$ to form NO^+ and $(N_2O \cdot NO)^+$, respectively, follow similar reaction pathways, further supporting the notion that ionization of the neutral N_2O dimer occurs on a single monomer unit to form $N_2O^+ \cdot N_2O$. The neutral monomer in $N_2O^+ \cdot N_2O$ then acts simply as a spectator in the fragmentation process leading to the formation of $(N_2O \cdot NO)^+$. Note that N_2O^+ may undergo another fragmentation process leading to the formation of $NO^+(X\,^1\Sigma^+)$ and $N(^2D)$. The thermochemical threshold for the formation of NO^+ by this process would be 16.57 eV,[16] suggesting that another break in the ionization efficiency curve of $(N_2O \cdot NO)^+$ may be expected between 14.3 and 17.0 eV. We were unable to detect this break, although there was some evidence for such a feature on the photoionization efficiency curve measured by Linn and Ng.[4] Our failure to observe this feature may be attributed to the low-energy resolution of the instrument employed for the present study. The fragmentation of $N_2O^+ \cdot N_2O$ may then be viewed as a set of energy-dependent unimolecular cluster ion dissociation reactions as shown in eqn. (4), analogous to eqn. (2) and (3).

$$\begin{aligned} &\text{—14.6 eV} \rightarrow && (N_2O)O^+ + N_2 + 2e^- \\ (N_2O)N_2O + e^- &\text{—14.3 eV} \rightarrow && (N_2O)NO^+ + N(^4S) + 2e^- \\ &\text{—16.6 eV} \rightarrow && (N_2O)NO^+ + N(^2D) + 2e^- \\ &\text{—17.0 eV} \rightarrow && (N_2O)NO^+ + N(^2P) + 2e^- \end{aligned} \quad (4)$$

NH_3 Clusters

Ionization efficiency curves for the ammonia clusters are shown in Fig. 4 and 5 and appearance energies are listed in Table 3 for $(NH_3)_nNH_4^+$ $(0 \leqslant n \leqslant 7)$. Discrepancies between binding energies deduced from ion–molecule equilibria and from cluster-ion appearance energies suggest that electron impact and photoionization fail to yield the true adiabatic ionization energies of these weakly bound species.[2,5] Dissociation energies of the $(NH_3)_nNH_4^+$ ions deduced from appearance energy measurements were found to be in poor

Table 3 Appearance energies (E_{app}) for $(NH_3)_nNH_4^+$ $(0 \leqslant n \leqslant 7)$

ion	E_{app}/eV	
	electron impact[a]	photoionization[b]
NH_4^+	9.7	9.59 ± 0.02
$(NH_3)NH_4^+$	9.2	9.15 ± 0.04
$(NH_3)_2NH_4^+$	9.0	9.03 ± 0.04
$(NH_3)_3NH_4^+$	8.9	—
$(NH_3)_4NH_4^+$	8.8_5	—
$(NH_3)_5NH_4^+$	8.8_1	—
$(NH_3)_6NH_4^+$	8.7_8	—
$(NH_3)_7NH_4^+$	8.7_2	—

[a] Reproducibility ±0.1 eV or better (this work). [b] Ref. 8.

accord with those obtained by ion–molecule methods, indicative of this failure of electron impact ionization measurements to sample the true adiabatic ionization thresholds for the ammonia cluster ions.

Conclusion

Klots and Compton[2] suggested that the equilibrium geometry of van der Waals cluster ions produced by electron impact or photoionization may be considerably different from the equilibrium geometry of the neutral precursor. In such situations the Franck–Condon factors near the true adiabatic ionization threshold may be so small that the observation of the adiabatic threshold is precluded. It has been suggested that small Franck–Condon factors near threshold are not a particularly serious problem in the ionization of rare-gas cluster species owing to the close spacing of many Rydberg levels throughout the region between the adiabatic and the direct ionization thresholds which may decay *via* autoionization.[8,19] Rydberg states with lifetimes greater than 50 μs and principal quantum numbers $55 \leqslant n \leqslant 75$ have been reported for CO_2 clusters by Campbell and Tittes.[20] Such long-lived high Rydberg states can be observed only if there are some states for which non-radiative mechanisms of decay, such as autoionization and electronic predissociation, are significantly slower than radiative decay. It has been shown[21] that predissociation rates of molecular Rydberg states are considerably greater for states of low principal quantum number and while autoionization is the most probable non-radiative decay mechanism, the apparent absence of states with principal quantum number less than 55 observed in the experiment performed by Campbell and Tittes[20] indicates that predissociation may also be an important mechanism. It is therefore possible that lower Rydberg states of molecular clusters may, in fact, predissociate instead of decaying to levels of lower energy *via* the autoionization process. For this reason, unfavourable Franck–Condon factors may not be completely compensated for in the ionization of molecular cluster species, making the observation of their true adiabatic ionization potentials unlikely. Some knowledge of Franck–Condon factors for van der Waals clusters may therefore be required for the reliable interpretation of cluster-ion appearance potentials. The most probable mechanism for the formation of the cluster fragment ions $(N_2O \cdot O)^+$ and $(N_2O \cdot NO)^+$ would appear to involve the ionization and fragmentation of one of the N_2O molecules in the neutral N_2O dimer without any significant perturbation of the second molecule, although alternative mechanisms cannot be discounted. Despite these recognised deficiencies, electron impact ionization efficiency curves can provide significant mechanistic information, especially where breaks are found and where comparisons with monomer measurements and data collected using other techniques are available.

References

1 M. Mautner and F. H. Field, *J. Chem. Phys.*, 1977, **66**, 4527.
2 C. E. Klots and R. N. Compton, *J. Chem. Phys.*, 1978, **69**, 1636.
3 G. G. Jones and J. W. Taylor, *J. Chem. Phys.*, 1978, **68**, 1768.
4 S. H. Linn and C. Y. Ng, *J. Chem. Phys.*, 1981, **75**, 4921.
5 K. Stephan, J. H. Futrell, K. I. Peterson, A. W. Castleman Jr. and T. D. Märk, *J. Chem. Phys.*, 1982, **77**, 2408.
6 B. Kamke, W. Kamke, R. Herrmann and I. V. Hertel, *Z. Phys. D*, 1989, **11**, 153.
7 K. Stephan, J. H. Futrell, K. I. Peterson, A. W. Castleman Jr., H. E. Wagner, N. Djuric and T. D. Märk, *J. Mass Spectrom.*, 1982, **44**, 167.
8 S. T. Ceyer, P. W. Tiedemann, B. H. Mahan and Y. T. Lee, *J. Chem. Phys.*, 1979, **70**, 14.
9 B. R. Cameron and P. W. Harland, *J. Chem. Soc., Faraday Trans.*, 1991, **87**, 1069.
10 *Atomic and Molecular Beam Methods*, ed. G. Scoles, Oxford University Press, London, 1988.
11 C. A. McDowell, *The Ionization and Dissociation of Molecules*, McGraw-Hill, New York, 1963.
12 R. W. Kiser, *Introduction to Mass Spectrometry and its Applications*, Prentice-Hall, Englewood Cliffs, NY, 1965.
13 V. H. Dibeler and R. M. Reese, *Adv. Mass Spectrom.*, 1966, **3**, 471.
14 R. G. Keese and A. W. Castleman, *J. Phys. Chem. Ref. Data*, 1986, **15**, 1011.
15 K. Hiraoka, G. Nakajima and S. Shoda, *Chem. Phys. Lett.*, 1988, **146**, 535.
16 H. M. Rosenstock, K. Draxl, B. W. Steiner and J. T. Herron, *J. Phys. Chem. Ref. Data 6, Suppl. 1*, 1977, **70**.
17 H. L. Johnston and K. E. McCloskey, *J. Phys. Chem.*, 1940, **44**, 1038.
18 A. J. Illies, *J. Phys. Chem.*, 1988, **92**, 2889.
19 C. Y. Ng, D. J. Trevor, P. W. Tiedemann, S. T. Ceyer, P. L. Kronebusch, B. H. Mahan and Y. T. Lee, *J. Chem. Phys.*, 1977, **62**, 4235.
20 E. E. B. Campbell and A. Tittes, *Chem. Phys. Lett.*, 1990, **165**, 289.
21 S. M. Tarr, J. A. Schiavone and R. S. Freund, *J. Chem. Phys.*, 1981, **74**, 2869.

Paper 3/05770D; *Received* 24*th September*, 1993